Curvature continuous corner cutting ☆

Kai Hormann [a,*], Claudio Mancinelli [b]

[a] *Faculty of Informatics, Università della Svizzera italiana, Switzerland*
[b] *DIBRIS, Università degli Studi di Genova, Italy*

A R T I C L E   I N F O

A B S T R A C T

Subdivision schemes are used to generate smooth curves by iteratively refining an initial control polygon. The simplest such schemes are corner cutting schemes, which specify two distinct points on each edge of the current polygon and connect them to get the refined polygon, thus cutting off the corners of the current polygon. While de Boor (1987) shows that this process always converges to a Lipschitz continuous limit curve, no matter how the points on each edge are chosen, Gregory and Qu (1996) discover that the limit curve is continuously differentiable under certain constraints. We extend these results and show that the limit curve can even be curvature continuous for specific sequences of cut ratios.

1. Introduction

Given a sequence of initial points $p_i^0 \in \mathbb{R}^2$, $i = 0, \dots, n+1$, we consider the general *corner cutting scheme* defined by the subdivision rules

$$p_{2i}^{k+1} = (1-\alpha_i^k)p_i^k + \alpha_i^k p_{i+1}^k, \qquad p_{2i+1}^{k+1} = \beta_i^k p_i^k + (1-\beta_i^k)p_{i+1}^k \qquad (1)$$

for $k = 0, 1, 2, \dots$ and $i = 0, \dots, 2^k n$, where

$$\alpha_i^k > 0, \qquad \beta_i^k > 0, \qquad 1 - \alpha_i^k - \beta_i^k > 0. \qquad (2)$$

Denoting by P_k the polygonal chain that is formed by connecting the points $p_0^k, \dots, p_{2^k n+1}^k$ with line segments, the corner cutting scheme (1) for creating P_{k+1} from P_k can be understood as follows. We first generate the points p_{2i}^{k+1} and p_{2i+1}^{k+1} by trisecting each line segment $[p_i^k, p_{i+1}^k]$ of P_k in the ratio $\alpha_i^k : 1 - \alpha_i^k - \beta_i^k : \beta_i^k$. We then keep the central pieces $[p_{2i}^{k+1}, p_{2i+1}^{k+1}]$, $i = 0, \dots, 2^k n$ of the trisected line segments and connect them with new line segments $[p_{2i-1}^{k+1}, p_{2i}^{k+1}]$, $i = 1, \dots, 2^k n$, which cut off the corners of P_k (see Fig. 1). Since the cut ratios α_i^k and β_i^k may depend on both k and i, this scheme is non-uniform in general.

Note that scheme (1) can also be applied to a closed initial control polygon with n vertices $p_1^0, \dots, p_n^0$ by simply setting $p_0^0 = p_n^0$ and $p_{n+1}^0 = p_1^0$ and making sure that $\alpha_0^k = \alpha_{2^k n}^k$ and $\beta_0^k = \beta_{2^k n}^k$ for $k \geq 0$, so that the first and the last segment of each P_k are identical and trisected in the same ratio.

Uniform corner cutting schemes with $\alpha_i^k = \beta_i^k = \omega > 0$ for all k and i date back to the work of de Rham (1947a,b), who studies the case $\omega = \frac{1}{3}$ and proves that the sequence (P_k) converges to a differentiable limit curve $P = \lim_{k \to \infty} P_k$. He later generalizes this

---
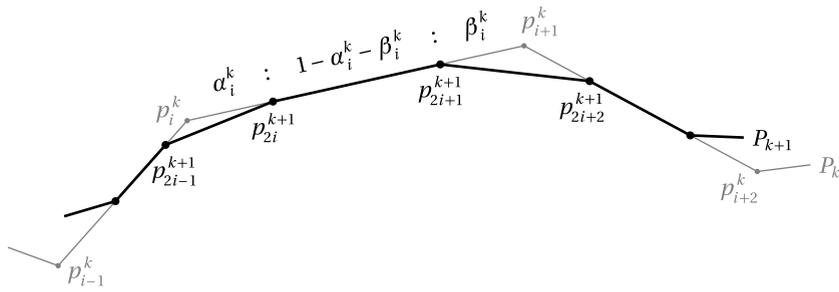
Fig. 1. The corner cutting scheme (1) creates the polygonal chain P_{k+1} from P_k by first trisecting each line segment $[p_i^k, p_{i+1}^k]$ of P_k in the ratio $\alpha_i^k : 1 - \alpha_i^k - \beta_i^k : \beta_i^k$ to give the new points p_{2i}^{k+1} and p_{2i+1}^{k+1}, and then replacing each corner $[p_{2i-1}^{k+1}, p_i^k, p_{2i}^{k+1}]$ with the line segment $[p_{2i-1}^{k+1}, p_{2i}^{k+1}]$.
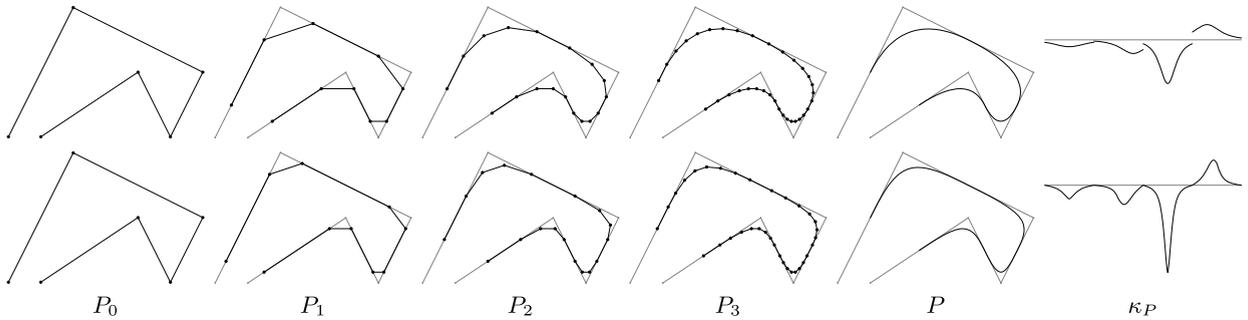
Fig. 2. Initial data, data generated by the first three subdivision steps, limit curve, and signed curvature of the limit curve (from left to right) for the uniform corner cutting scheme with $\omega = \frac{1}{4}$ (top) and the non-uniform corner cutting scheme with cut ratios in (5) (bottom).

result (de Rham, 1956) and shows that the limit curve P is continuous (C^0) for any $\omega < \frac{1}{2}$ and continuously differentiable (C^1) for any $\omega \le \frac{1}{3}$. He also discovers that P is a piecewise quadratic curve for $\omega = \frac{1}{4}$ (see Fig. 2, top), a fact that was independently observed by Chaikin (1974) and proven by Riesenfeld (1975), who more specifically notes that the limit curve is the quadratic B-spline with control points $p_0^0, \ldots, p_{n+1}^0$ and uniform knots $(-2, -1, \ldots, n + 2)$. For the asymmetric setting, where $\alpha_i^k = \alpha > 0$ and $\beta_i^k = \beta > 0$ for all k and i, de Rham (1959) further proves that P is C^0, if $\alpha + \beta < 1$ and C^1, if $2\alpha + \beta \le 1$ and $\alpha + 2\beta \le 1$.

Gregory and Qu (1996) generalize de Rham's results to the *non-uniform* setting, where the cut ratios may depend on k and i, and show that the limit curve is C^0, if

$$\underline{\alpha} > 0, \qquad \underline{\beta} > 0, \qquad \overline{\alpha} + \overline{\beta} < 1, \tag{3}$$

and C^1, if

$$\underline{\alpha} > 0, \qquad \underline{\beta} > 0, \qquad 2\overline{\alpha} + \overline{\beta} < 1, \qquad \overline{\alpha} + 2\overline{\beta} < 1, \tag{4}$$

where

$$\underline{\alpha} = \varliminf_{k \to \infty} \min_i \alpha_i^k, \qquad \overline{\alpha} = \varlimsup_{k \to \infty} \max_i \alpha_i^k, \qquad \underline{\beta} = \varliminf_{k \to \infty} \min_i \beta_i^k \qquad \overline{\beta} = \varlimsup_{k \to \infty} \max_i \beta_i^k.$$

Even more general corner cutting processes were studied by de Boor, who proves that they always work in the sense that the sequence of generated polygonal chains converges uniformly to a Lipschitz continuous curve (de Boor, 1987). Moreover, he shows that the limit curve is C^1 if all the corners of the polygonal chain flatten out in the limit (de Boor, 1990), similar to how de Rham (1947a,b) establishes the tangent continuity of the limit curve in the symmetric uniform case with $\omega = \frac{1}{3}$, and presents an example to illustrate that this condition is not necessary. Paluszny et al. (1997) improve these results by providing a sufficient and necessary condition for a corner cutting process to generate a C^1 limit curve and by pointing out that condition (4) is not necessary. More recent work analyses non-uniform corner cutting schemes with local tension parameters (Fang et al., 2017) and for generating exponential B-splines (Jeong et al., 2021), and in both cases the limit curves are shown to be C^1.

1.1. Contribution

So far, there exists no corner cutting scheme that generates curvature continuous (G^2) limit curves. The goal of this paper is to derive such schemes. For example, the non-uniform scheme with cut ratios
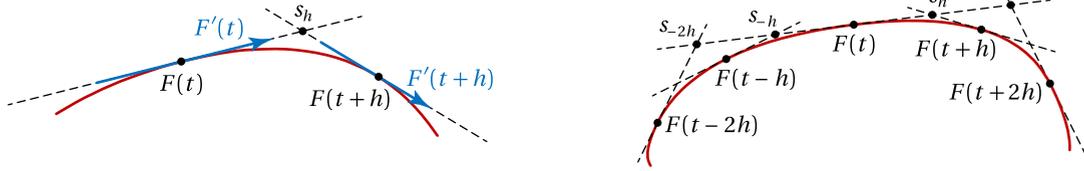
Fig. 3. Notation used in Proposition 1 (left) and Proposition 2 (right).

$$\alpha_i^k = \begin{cases} \frac{1}{6}, & \text{if } k = 0, \\ \frac{1}{4}, & \text{if } j_i^k = 0, \\ \upsilon(-j_i^k), & \text{if } j_i^k = -2^{k-1}, \\ \omega(j_i^k), & \text{otherwise,} \end{cases} \qquad \beta_i^k = \begin{cases} \frac{1}{6}, & \text{if } k = 0, \\ \frac{1}{4}, & \text{if } j_i^k = 0, \\ \upsilon(-j_i^k), & \text{if } j_i^k = -2^{k-1}, \\ \omega(-j_i^k), & \text{otherwise.} \end{cases} \tag{5}$$

for $k \geq 0$ and $i = 0, \ldots, 2^k n$, where

$$j_i^k = \left((i + 2^{k-1}) \bmod 2^k \right) - 2^{k-1} \tag{6}$$

and

$$\upsilon(j) = \frac{6j^2 - 6j + 1}{2(3j - 2)(4j - 1)}, \qquad \omega(j) = \frac{(6j^2 - 6j + 1)(2j + 1)}{4(3j^2 - 1)(4j - 1)}, \tag{7}$$

generates G^2 limit curves (see Fig. 2, bottom). In Section 2 we explain how to derive the cut ratios in (5), and we extend this basic scheme in two different directions in Sections 3 and 4.

2. The basic scheme

The reason why the non-uniform corner cutting scheme with cut ratios in (5) generates G^2 limit curves is rather simple: the limit curve is the C^2 cubic B-spline $B : [0, 2n] \to \mathbb{R}^2$ with $2n + 3$ control points

$$p_0^0, \quad \tfrac{1}{2}(p_0^0 + p_1^0), \quad p_1^0, \quad \tfrac{1}{2}(p_1^0 + p_2^0), \quad p_2^0, \quad \cdots \quad p_n^0, \quad \tfrac{1}{2}(p_n^0 + p_{n+1}^0), \quad p_{n+1}^0 \tag{8}$$

and uniform knots $(-3, -2, \ldots, 2n + 3)$. To prove this property, we recall an important feature of any corner cutting algorithm, namely that the limit curve is tangent to all line segments of the polygonal chain P_k at all levels k. In turn, this implies that every point p_i^k is the intersection of two lines that are tangent to the limit curve. Before applying this observation to our basic scheme, let us first study such intersection points in general.

Proposition 1. *Given a differentiable parametric planar curve $F : \mathbb{R} \to \mathbb{R}^2$ and some $t \in \mathbb{R}$, the intersection point s_h of the lines tangent to the curve at $F(t)$ and $F(t + h)$ for any $h \neq 0$ (see Fig. 3, left) exists and can be expressed as*

$$s_h = F(t) + \lambda_h F'(t), \qquad \lambda_h = \frac{\det\left(F(t + h) - F(t), F'(t + h)\right)}{\det\left(F'(t), F'(t + h)\right)}, \tag{9}$$

as long as the two tangent lines are not parallel.

Proof. If the two tangent lines are not parallel, then $\det\left(F'(t), F'(t + h)\right) \neq 0$ and there exist $\lambda_h, \mu_h \in \mathbb{R}$, such that $s_h = F(t) + \lambda_h F'(t)$ and $s_h = F(t + h) + \mu_h F'(t + h)$. Therefore,

$$\lambda_h F'(t) = F(t + h) - F(t) + \mu_h F'(t + h)$$

and further

$$\det\left(\lambda_h F'(t), F'(t + h)\right) = \det\left(F(t + h) - F(t) + \mu_h F'(t + h), F'(t + h)\right),$$

which, after solving for λ_h, gives (9), because $\det\left(F'(t + h), F'(t + h)\right) = 0$. $\square$

Proposition 2. *Given a differentiable parametric planar curve $F : \mathbb{R} \to \mathbb{R}^2$ and some $t \in \mathbb{R}$ and assuming that the intersection points s_{-2h}, s_{-h}, s_h, s_{2h} of the tangent line at $F(t)$ with the tangent lines at $F(t - 2h)$, $F(t - h)$, $F(t + h)$, $F(t + 2h)$ exist uniquely and that $s_{-2h} \neq s_{2h}$ (see Fig. 3, right), s_{-h} and s_h can be expressed as affine combinations of s_{-2h} and s_{2h},*

$$s_{-h} = (1 - \alpha)\, s_{-2h} + \alpha\, s_{2h}, \qquad s_h = \beta\, s_{-2h} + (1 - \beta)\, s_{2h},$$

where
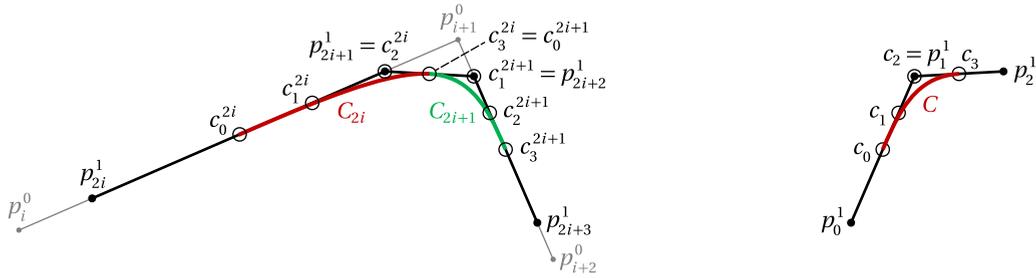
Fig. 4. Bézier control points c_m^j, $m = 0, 1, 2, 3$ of the cubic pieces C_j of the limit curve for $j = 2i$ and $j = 2i + 1$ (left) and simplified notation for the first piece of the limit curve (right).

$$\alpha = \frac{\lambda_{-h} - \lambda_{-2h}}{\lambda_{2h} - \lambda_{-2h}}, \qquad \beta = \frac{\lambda_{2h} - \lambda_h}{\lambda_{2h} - \lambda_{-2h}}.$$

Proof. By (9), the intersection points s_{-2h}, s_{-h}, s_h, s_{2h} are the images of λ_{-2h}, λ_{-h}, λ_h, λ_{2h} under the affine map $\phi(\lambda) = F(t) + \lambda F'(t)$. The statement then follows from the fact that

$$\lambda_{-h} = (1 - \alpha) \lambda_{-2h} + \alpha \lambda_{2h}, \qquad \lambda_h = \beta \lambda_{-2h} + (1 - \beta) \lambda_{2h},$$

which can be verified easily. $\square$

Now it is time to go back to the limit curve of our basic scheme, the uniform cubic B-spline B with control points in (8). Converting this curve to piecewise Bézier form (Goldman, 2003, Section 7.6.3.1), we find that the control points $c_0^j, c_1^j, c_2^j, c_3^j$ of its $2n$ cubic pieces $C_j : [j, j+1] \to \mathbb{R}^2$, $j = 0, \dots, 2n - 1$ are

$$c_0^{2i} = \tfrac{1}{2}(p_i^0 + p_{i+1}^0), \qquad\qquad c_0^{2i+1} = \tfrac{1}{12}(p_i^0 + 10p_{i+1}^0 + p_{i+2}^0),$$
$$c_1^{2i} = \tfrac{1}{3}(p_i^0 + 2p_{i+1}^0), \qquad\qquad c_1^{2i+1} = \tfrac{1}{6}(5p_{i+1}^0 + p_{i+2}^0),$$
$$c_2^{2i} = \tfrac{1}{6}(p_i^0 + 5p_{i+1}^0), \qquad\qquad c_2^{2i+1} = \tfrac{1}{3}(2p_{i+1}^0 + p_{i+2}^0),$$
$$c_3^{2i} = \tfrac{1}{12}(p_i^0 + 10p_{i+1}^0 + p_{i+2}^0), \qquad c_3^{2i+1} = \tfrac{1}{2}(p_{i+1}^0 + p_{i+2}^0),$$

for $i = 0, \dots, n - 1$ (see Fig. 4, left). Note that

$$c_1^{2i} = \tfrac{1}{2}(c_0^{2i} + c_2^{2i}), \qquad c_3^{2i} = \tfrac{1}{2}(c_2^{2i} + c_1^{2i+1}) = c_0^{2i+1}, \qquad c_2^{2i+1} = \tfrac{1}{2}(c_1^{2i+1} + c_3^{2i+1})$$

and that the cut ratios in (5) for $k = 0$ are chosen such that

$$c_2^{2i} = p_{2i+1}^1, \qquad c_1^{2i+1} = p_{2i+2}^1.$$

Let us now focus on the first piece of the limit curve and omit the piece index $j = 0$ for simplicity. That is, we consider the cubic Bézier curve $C : [0, 1] \to \mathbb{R}$ with control points

$$c_0 = \tfrac{1}{2}(p_0^1 + p_1^1), \qquad c_1 = \tfrac{1}{2}(c_0 + c_2), \qquad c_2 = p_1^1, \qquad c_3 = \tfrac{1}{2}(p_1^1 + p_2^1), \qquad (10)$$

shown in Fig. 4 (right). As C is tangent to the line segments $[p_0^1, p_1^1]$ and $[p_1^1, p_2^1]$ at its endpoints, we observe that p_1^1 is the intersection point of the tangent lines at $C(0)$ and $C(1)$. More generally, we will see that the points p_i^k generated by the corner cutting scheme with cut ratios in (5) are the intersection points of lines tangent to C at certain dyadic points, but we first need to simplify the statement of Proposition 1 for this specific curve C.

Corollary 3. *Given the cubic Bézier curve $C : [0, 1] \to \mathbb{R}$ with control points in (10) and some $t \in [0, 1]$, the intersection point s_h of the lines tangent to the curve at $C(t)$ and $C(t + h)$ for any $h \neq 0$ with $t + h \in [0, 1]$ exists and can be expressed as*

$$s_h = C(t) + \lambda_h C'(t), \qquad \lambda_h = \frac{h(3t + 2h)}{3(2t + h)}, \qquad (11)$$

as long as p_0^0, p_1^0, and p_2^0 are not collinear.

Proof. By the properties of Bézier curves (Goldman, 2003, Section 5.6.2),

$$C'(t) = 3(c_1 - c_0)(1 - t)^2 + 6(c_2 - c_1)(1 - t)t + 3(c_3 - c_2)t^2,$$
$$C''(t) = 6(c_2 - 2c_1 + c_0)(1 - t) + 6(c_3 - 2c_2 + c_1)t,$$
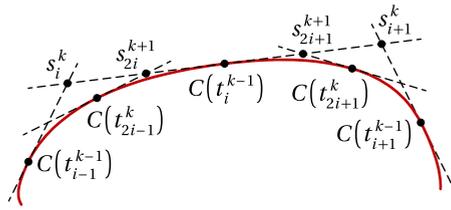
Fig. 5. Notation used in Corollary 4.

$$C'''(t) = 6(c_3 - 3c_2 + 3c_1 - c_0),$$

and after substituting $c_1 = \frac{1}{2}(c_0 + c_2)$, we find that

$$C'(t) = \frac{3}{2}(c_2 - c_0) + \frac{1}{2}t^2 C'''(t),$$
$$C''(t) = t\, C'''(t), \tag{12}$$
$$C'''(t) = 6(c_3 - c_2) - 3(c_2 - c_0).$$

As C is a cubic curve, we have, by Taylor expansion,

$$C(t+h) = C(t) + hC'(t) + \frac{1}{2}h^2 C''(t) + \frac{1}{6}h^3 C'''(t)$$
$$= C(t) + hC'(t) + \frac{1}{6}(3t+h)h^2 C'''(t)$$

and

$$C'(t+h) = C'(t) + hC''(t) + \frac{1}{2}h^2 C'''(t)$$
$$= C'(t) + \frac{1}{2}(2t+h)hC'''(t).$$

Inserting both into the formula for λ_h in (9) and abbreviating $C'(t)$, $C''(t)$, $C'''(t)$ by C', C'', C''', we get

$$\lambda_h = \frac{\det\left(hC' + \frac{1}{6}(3t+h)h^2 C''', C' + \frac{1}{2}(2t+h)hC'''\right)}{\det\left(C', C' + \frac{1}{2}(2t+h)hC'''\right)} = \frac{\frac{1}{6}\left(3(2t+h) - (3t+h)\right)h^2 \det(C', C''')}{\frac{1}{2}(2t+h)h\det(C', C''')},$$

which simplifies to the expression for λ_h in (11) after cancelling $h \neq 0$ and $\det(C', C''')$. The latter is valid, because (10) and (12) imply that

$$\det(C', C''') = 9\det(c_2 - c_0, c_3 - c_2) = \frac{9}{4}\det\left(p_1^1 - p_0^1, p_2^1 - p_1^1\right),$$

which vanishes if and only if p_0^0, p_1^0, and p_2^0 are collinear. Note that the conditions on t and h guarantee that $(2t+h) \neq 0$, so that λ_h is finite. $\quad\square$

Corollary 4. *Given the cubic Bézier curve $C : [0,1] \to \mathbb{R}$ with control points in (10) and assuming that p_0^0, p_1^0, and p_2^0 are not collinear, the intersection point s_i^k of the tangent lines at $C\left(t_{i-1}^{k-1}\right)$ and $C\left(t_i^{k-1}\right)$, where $t_i^k = i/2^k$, is identical to the point p_i^k generated by the corner cutting scheme with cut ratios in (5) for $k \geq 1$ and $i = 1, \ldots, 2^{k-1}$ (see Fig. 5).*

Proof. We first note that all intersection points exist by Corollary 3. We then prove the statement by induction over k and recall that the base case ($k = 1$, $i = 1$) was already observed above (see Fig. 4, right). For the inductive step, we use Proposition 2 with $h = 1/2^k$ and $t = t_i^{k-1} = 2ih$, hence

$$\lambda_{-2h} = -\frac{2(3i-2)}{3(2i-1)}h, \qquad \lambda_{-h} = -\frac{2(3i-1)}{3(4i-1)}h, \qquad \lambda_h = \frac{2(3i+1)}{3(4i+1)}h, \qquad \lambda_{2h} = \frac{2(3i+2)}{3(2i+1)}h,$$

by (11), to conclude that

$$s_{2i}^{k+1} = (1-\alpha)p_i^k + \alpha p_{i+1}^k, \qquad\qquad s_{2i+1}^{k+1} = \beta p_i^k + (1-\beta)p_{i+1}^k,$$

for $i = 1, \ldots, 2^{k-1} - 1$, where

$$\alpha = \frac{\lambda_{-h} - \lambda_{-2h}}{\lambda_{2h} - \lambda_{-2h}} = \frac{-\frac{(3i-1)}{(4i-1)} + \frac{(3i-2)}{(2i-1)}}{\frac{(3i+2)}{(2i+1)} + \frac{(3i-2)}{(2i-1)}} = \omega(i), \qquad\qquad \beta = \frac{\lambda_{2h} - \lambda_h}{\lambda_{2h} - \lambda_{-2h}} = \frac{\frac{(3i+2)}{(2i+1)} - \frac{(3i+1)}{(4i+1)}}{\frac{(3i+2)}{(2i+1)} + \frac{(3i-2)}{(2i-1)}} = \omega(-i),$$

which are equal to α_i^k and β_i^k in (5), because $j_i^k = i$.

It remains to show the statement for p_1^{k+1} and $p_{2^k}^{k+1}$. We start with p_1^{k+1}. On the one hand, using $h = 1/2^k$ and $t = 0$ in Corollary 3, we find that $s_1^k = C(0) + \lambda_{2h}C'(0)$ and $s_1^{k+1} = C(0) + \lambda_h C'(0)$, hence

$$s_1^{k+1} = (1-\mu)C(0) + \mu s_1^k = (1-\mu)c_0 + \mu p_1^k, \qquad \mu = \frac{\lambda_h}{\lambda_{2h}} = \frac{1}{2}.$$

On the other hand, since $\alpha_0^k = \beta_0^k = \frac{1}{4}$ for $k \geq 1$ implies $c_0 = \frac{1}{2}(p_0^k + p_1^k)$, we have

$$p_1^{k+1} = \beta_0^k p_0^k + (1-\beta_0^k)p_1^k = (1-\tfrac{1}{2})c_0 + \tfrac{1}{2}p_1^k$$

and therefore $p_1^{k+1} = s_1^{k+1}$. Similarly, using $h = 1/2^k$ and $t = 1$ in Corollary 3, we get

$$s_{2^k}^{k+1} = (1-\mu)C(1) + \mu s_{2^k-1}^k = (1-\mu)c_3 + \mu p_{2^k-1}^k, \qquad \mu = \frac{\lambda_{-h}}{\lambda_{-2h}} = \frac{(3-2h)(1-h)}{(2-h)(3-4h)},$$

and since $\alpha_{2^k-1}^k = \beta_{2^k-1}^k = \upsilon(2^{k-1})$ for $k \geq 1$ implies $c_3 = \frac{1}{2}(p_{2^k-1}^k + p_{2^k-1+1}^k)$, we have

$$p_{2^k}^{k+1} = (1-\alpha_{2^k-1}^k)p_{2^k-1}^k + \alpha_{2^k-1}^k p_{2^k-1+1}^k = (1-2\upsilon(2^{k-1}))p_{2^k-1}^k + 2\upsilon(2^{k-1})c_3$$

and consequently $p_{2^k}^{k+1} = s_{2^k}^{k+1}$, because

$$\upsilon(2^{k-1}) = \upsilon(\tfrac{1}{2h}) = \frac{\frac{6}{4h^2} - \frac{6}{2h} + 1}{2(-\frac{4}{2h}+1)(-\frac{3}{2h}+2)} = \frac{3 - 6h + 2h^2}{2(2-h)(3-4h)} = \frac{1-\mu}{2}. \quad \square$$

To extend Corollary 4 to the other cubic pieces C_m of the B-spline B, observe that the points p_i^k corresponding to C_m are those with indices $k \geq 1$ and $i = 2^{k-1}m + l$ for $l = 1, \ldots, 2^{k-1}$. If m is even, then any such i is mapped to the local index j_i^k in (6) exactly as in the case $m = 0$, namely $j_i^k = l$ for $l = 1, \ldots, 2^{k-1}-1$ and $j_i^k = -2^{k-1}$ for $l = 2^{k-1}$, and the proof remains the same, because $(\alpha_i^k, \beta_i^k) = (\alpha_l^k, \beta_l^k)$. The situation is slightly different for odd m, since $c_2^m = \frac{1}{2}(c_1^m + c_3^m)$ in this case, while $c_1^m = \frac{1}{2}(c_0^m + c_2^m)$ for even m. We thus need to "mirror" the indices and ensure that the cut ratios (α_i^k, β_i^k) are identical to $(\beta_{2^{k-1}-l}^k, \alpha_{2^{k-1}-l}^k)$. But this is exactly the reason for the definition of j_i^k. If m is odd, then i is mapped to $j_i^k = l - 2^{k-1}$, so that $\alpha_i^k = \omega(j_i^k) = \omega(-(2^{k-1}-l)) = \beta_{2^{k-1}-l}^k$ and similarly for β_i^k.

We are now ready to wrap up our results and prove that our basic scheme generates G^2 limit curves.

Theorem 5. *The sequence of polygons (P_k) generated by the corner cutting scheme with cut ratios in (5) converges to the uniform cubic B-spline B with control points in (8) and thus to a curvature continuous limit curve.*

Proof. On the one hand, it is straightforward to show that $\upsilon(j)$ and $\omega(j)$ in (7) are strictly increasing for $j \geq 1$ with $\upsilon(1) = \frac{1}{6}$, $\omega(1) = \frac{1}{8}$, and $\lim_{j \to \infty} \upsilon(j) = \lim_{j \to \infty} \omega(j) = \frac{1}{4}$. Similarly, $\omega(-j)$ is strictly decreasing with $\omega(-1) = \frac{13}{40}$ and $\lim_{j \to \infty} \omega(-j) = \frac{1}{4}$. Therefore, $\underline{\alpha} = \underline{\beta} = \frac{1}{8}$ and $\overline{\alpha} = \overline{\beta} = \frac{13}{40}$, so that the Gregory–Qu condition (4) is satisfied and the limit curve $P = \lim_{k \to \infty} P_k$ is guaranteed to be C^1.

On the other hand, it follows from Corollary 4 that P_k for $k \geq 1$ agrees with the first cubic piece C_0 of the limit curve B at the dyadic points t_i^{k-1} for $i = 0, \ldots, 2^{k-1}$ and, as explained above, the same holds for the other cubic pieces C_j, $j = 1, \ldots, 2n-1$ and the dyadic points t_i^{k-1} for $i = 2^{k-1}, \ldots, 2^k n$. Therefore, P agrees with B on the dense set of dyadic points in $[0, 2n]$, and as P is continuous, it must be identical to B, which is G^2, because it is C^2 and regular.

Note that the case of collinear points p_0^0, p_1^0, and p_2^0 that we excluded in Corollary 4 can be dealt with by a continuity argument. Just move p_1^0 by some $\varepsilon > 0$ in a direction that is not parallel to $p_2^0 - p_0^0$, so that the three points are not collinear anymore and the convergence of (P_k) to B follows as above, and then let $\varepsilon \to 0$. $\square$

We can further show that the convergence order of our basic scheme is quadratic.

Proposition 6. *The distance between B and P_k is on the order of h^2, where $h = 1/2^k$.*

Proof. Without loss of generality, we focus again on the first piece of B, that is, the cubic Bézier curve C with control points in (10), and more specifically on the interval $[t, t+h]$, where $t = t_{i-1}^{k-1} \in [0, 1)$ for some $k \geq 1$ and some $i \in \{1, \ldots, 2^{k-1}\}$ and $h = 1/2^k$. From Corollaries 3 and 4 we know that

$$p_i^k = C(t) + \lambda_{2h}C'(t), \qquad \lambda_{2h} = \frac{h(3t+4h)}{3(t+h)} \in \left[h, \tfrac{4}{3}h\right],$$
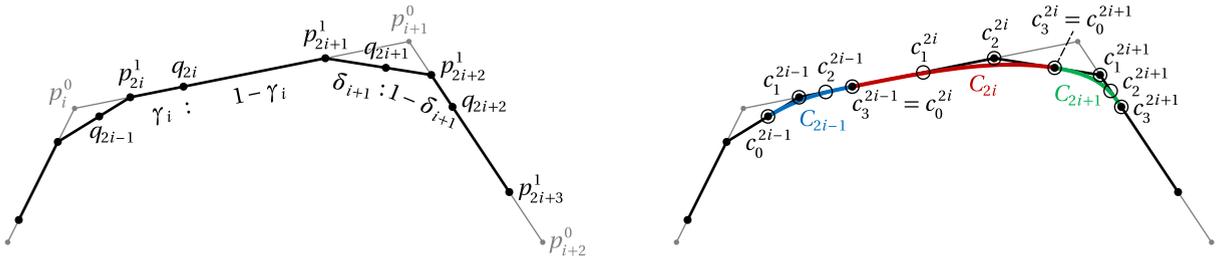
Fig. 6. After an initial corner cutting step with cut ratios $\alpha_i^0 = \alpha_i$ and $\beta_i^0 = \beta_i$ (cf. Fig. 1), we divide the line segments $\left[p_{2i}^1, p_{2i+1}^1\right]$ and $\left[p_{2i+1}^1, p_{2i+2}^1\right]$ of P_1 in the ratios $\gamma_i : 1 - \gamma_i$ and $\delta_{i+1} : 1 - \delta_{i+1}$, respectively (left) and then define the control points c_m^j, $m = 0, 1, 2, 3$ of the cubic Bézier curves C_j (right).

and that the line segment from $C(t)$ to p_i^k is a part of P_k (cf. Fig. 5). For any $s \in [t, t + h]$, consider the distance between $C(s)$ and the point $(1 - \mu)C(t) + \mu p_i^k$ on P_k, where $\mu = (s - t)/\lambda_{2h} \in [0, h/\lambda_{2h}] \subset [0, 1]$. By Taylor expansion,

$$C(s) = C(t + \mu\lambda_{2h}) = C(t) + \mu\lambda_{2h}C'(t) + \frac{(\mu\lambda_{2h})^2}{2}C''(t) + \frac{(\mu\lambda_{2h})^3}{6}C'''(t),$$

and therefore

$$C(s) - \left((1 - \mu)C(t) + \mu p_i^k\right) = \frac{(\mu\lambda_{2h})^2}{2}C''(t) + \frac{(\mu\lambda_{2h})^3}{6}C'''(t),$$

which is on the order of h^2, because λ_{2h} is on the order of h. By symmetry, we can similarly bound the distance between $C(s)$ for $s \in [t + h, t + 2h]$ and some point on P^k between p_i^k and $C(t + 2h) = C(t_i^{k-1})$, thus covering the whole domain $[0, 1]$ of C. $\quad\square$

3. Curvature continuous cubic Bézier splines

While the basic scheme with cut ratios in (5) generates a uniform cubic B-spline in the limit, that is, a piecewise cubic C^2 curve, we can modify it slightly, so that the sequence (P_k) converges to a more general G^2 cubic Bézier spline, also called γ-*spline* (Prautzsch et al., 2002, Section 7.3). To this end, suppose we are given α_i, β_i, and γ_i with

$$\alpha_i > 0, \qquad \beta_i > 0, \qquad \gamma_i > 0, \qquad 1 - \gamma_i > 0, \qquad 1 - \alpha_i - \beta_i > 0, \tag{13}$$

for $i = 0, \ldots, n$, and define

$$\delta_{i+1} = \frac{\alpha_{i+1}(1 - \gamma_i)(1 - \alpha_i - \beta_i) - \sqrt{\alpha_{i+1}\beta_i(1 - \gamma_i)\gamma_{i+1}(1 - \alpha_i - \beta_i)(1 - \alpha_{i+1} - \beta_{i+1})}}{\alpha_{i+1}(1 - \gamma_i)(1 - \alpha_i - \beta_i) - \beta_i\gamma_{i+1}(1 - \alpha_{i+1} - \beta_{i+1})}, \tag{14a}$$

if the denominator $\alpha_{i+1}(1 - \gamma_i)(1 - \alpha_i - \beta_i) - \beta_i\gamma_{i+1}(1 - \alpha_{i+1} - \beta_{i+1})$ does not vanish, and otherwise

$$\delta_{i+1} = \frac{1}{2}, \tag{14b}$$

for $i = 0, \ldots, n - 1$. We now use α_i and β_i as cut ratios for the first step of the corner cutting scheme, resulting in the polygonal chain P_1 with points

$$p_{2i}^1 = (1 - \alpha_i)p_i^0 + \alpha_i p_{i+1}^0, \qquad p_{2i+1}^1 = \beta_i p_i^0 + (1 - \beta_i)p_{i+1}^0, \tag{15}$$

for $i = 0, \ldots, n$. We then divide the line segments $\left[p_{2i}^1, p_{2i+1}^1\right]$ in the ratios $\gamma_i : 1 - \gamma_i$ and the line segments $\left[p_{2i+1}^1, p_{2i+2}^1\right]$ in the ratios $\delta_{i+1} : 1 - \delta_{i+1}$ to define the points $q_0, \ldots, q_{2n}$ as (see Fig. 6, left)

$$q_{2i} = (1 - \gamma_i)p_{2i}^1 + \gamma_i p_{2i+1}^1, \qquad q_{2i+1} = (1 - \delta_{i+1})p_{2i+1}^1 + \delta_{i+1}p_{2i+2}^1 \tag{16}$$

and consider the cubic Bézier spline $B : [0, 2n] \to \mathbb{R}^2$ that consists of the $2n$ cubic pieces $C_j : [j, j + 1] \to \mathbb{R}^2$, $j = 0, \ldots, 2n - 1$ with control points

$$\begin{aligned}
c_0^{2i} &= q_{2i}, & c_0^{2i+1} &= q_{2i+1}, \\
c_1^{2i} &= \tfrac{1}{2}(c_0^{2i} + c_2^{2i}), & c_1^{2i+1} &= p_{2i+2}^1, \\
c_2^{2i} &= p_{2i+1}^1, & c_2^{2i+1} &= \tfrac{1}{2}(c_1^{2i+1} + c_3^{2i+1}), \\
c_3^{2i} &= q_{2i+1}, & c_3^{2i+1} &= q_{2i+2},
\end{aligned} \tag{17}$$

for $i = 0, \ldots, n - 1$ (see Fig. 6, right).

Proposition 7. *The cubic Bézier spline B with control points in* (17) *is curvature continuous.*

Proof. Since $c_1^{2i-1}, c_2^{2i-1}, c_3^{2i-1} = c_0^{2i}, c_1^{2i}, c_2^{2i}$ are collinear, it is clear that the cubic Bézier curves C_{2i-1} and C_{2i}, for $i = 1, \ldots, n$, join curvature continuously with zero curvature (see Fig. 6, right). Moreover, for $i = 0, \ldots, n-1$, the curves C_{2i} and C_{2i+1} join tangent continuously (that is, G^1), because $c_2^{2i}, c_3^{2i} = c_0^{2i+1}, c_1^{2i+1}$ are collinear (see Fig. 6, right). To verify that the joint is also G^2, we recall from Farin (2002, Section 11.2) that this is the case, if and only if $r^2 = r_- r_+$, where

$$r = \frac{\|c_3^{2i} - c_2^{2i}\|}{\|c_1^{2i+1} - c_0^{2i+1}\|} = \frac{\delta_{i+1}}{1 - \delta_{i+1}},$$

$$r_- = \frac{\|c_2^{2i} - c_1^{2i}\|}{\|p_{i+1}^0 - c_2^{2i}\|} = \frac{\frac{1}{2}(1 - \gamma_i)(1 - \alpha_i - \beta_i)}{\beta_i},$$

$$r_+ = \frac{\|c_1^{2i+1} - p_{i+1}^0\|}{\|c_2^{2i+1} - c_1^{2i+1}\|} = \frac{\alpha_{i+1}}{\frac{1}{2}\gamma_{i+1}(1 - \alpha_{i+1} - \beta_{i+1})}.$$

Letting

$$\rho = \alpha_{i+1}(1 - \gamma_i)(1 - \alpha_i - \beta_i) \qquad \text{and} \qquad \sigma = \beta_i \gamma_{i+1}(1 - \alpha_{i+1} - \beta_{i+1}),$$

the G^2 condition is thus satisfied, if and only if δ_{i+1} solves

$$\left(\frac{\delta_{i+1}}{1 - \delta_{i+1}}\right)^2 = \frac{\rho}{\sigma} \qquad \Longleftrightarrow \qquad (\rho - \sigma)\delta_{i+1}^2 - 2\rho\delta_{i+1} + \rho = 0.$$

Note that $0 < \rho, \sigma < 1$, because of (13). If $\rho = \sigma$, then the only solution is $\delta_{i+1} = \frac{1}{2}$, as in (14b). Otherwise,

$$\delta_{i+1} = \frac{\rho - \sqrt{\rho\sigma}}{\rho - \sigma} \qquad \text{or} \qquad \delta_{i+1} = \frac{\rho + \sqrt{\rho\sigma}}{\rho - \sigma},$$

but only the first solution, which is the one in (14a), is guaranteed to be strictly between 0 and 1. Indeed, if $\sigma < \rho$, then $\sigma < \sqrt{\rho\sigma} < \rho$ and $0 < \frac{\rho - \sqrt{\rho\sigma}}{\rho - \sigma} < 1$, but $\frac{\rho + \sqrt{\rho\sigma}}{\rho - \sigma} > 1$. Likewise, if $\rho < \sigma$, then $\rho < \sqrt{\rho\sigma} < \sigma$ and $0 < \frac{\rho - \sqrt{\rho\sigma}}{\rho - \sigma} < 1$, but $\frac{\rho + \sqrt{\rho\sigma}}{\rho - \sigma} < 0$. $\square$

The G^2 cubic Bézier spline B now turns out to be generated in the limit by the non-uniform corner cutting scheme with cut ratios

$$\alpha_i^k = \begin{cases} \alpha_i, & \text{if } k = 0, \\ \frac{1}{2}\gamma_{l_i^k - 1}, & \text{if } j_i^k = 0, \\ 2\delta_{l_i^k}\upsilon(-j_i^k), & \text{if } j_i^k = -2^{k-1}, \\ \omega(j_i^k), & \text{otherwise}, \end{cases} \qquad \beta_i^k = \begin{cases} \beta_i, & \text{if } k = 0, \\ \frac{1}{2}(1 - \gamma_{l_i^k - 1}), & \text{if } j_i^k = 0, \\ 2(1 - \delta_{l_i^k})\upsilon(-j_i^k), & \text{if } j_i^k = -2^{k-1}, \\ \omega(-j_i^k), & \text{otherwise}. \end{cases} \qquad (18)$$

for $k \geq 0$ and $i = 0, \ldots, 2^k n$, where j_i^k, $\upsilon(j)$, and $\omega(j)$ are defined as in (6) and (7), respectively, and

$$l_i^k = \frac{i - (i \bmod 2^k)}{2^k} + 1. \qquad (19)$$

Note that l_i^k is used in the definition of the cut ratios only if $j_i^k = 0$ or $j_i^k = -2^{k-1}$. The first case occurs if and only if $i = 2^{k-1}(2m)$ and corresponds to the repeated trisection of the initial line segments $[p_m^0, p_{m+1}^0]$, $m = 0, \ldots, n$. In this case, $l_i^k - 1 = m$ and α_i^k, β_i^k are defined to clip off exactly half of the line segment to the left and to the right of q_{2m}, so that q_{2m} keeps dividing the remaining line segment in the ratio $\gamma_m : 1 - \gamma_m$. Similarly, the second case, which happens if and only if $i = 2^{k-1}(2m + 1)$, corresponds to the line segment $[p_{2m+1}^1, p_{2m+2}^1]$, $m = 0, \ldots, n-1$ and guarantees that q_{2m+1} keeps dividing the remnants of this line segment in the ratio $\delta_{m+1} : 1 - \delta_{m+1}$.

Theorem 8. *The sequence of polygons (P_k) generated by the corner cutting scheme with cut ratios in (18) converges to the cubic Bézier spline B with control points in (17) and thus to a curvature continuous limit curve.*

Proof. We proceed as in the proof of Theorem 5 and first observe that

$$\underline{\alpha} = \min\left\{\tfrac{1}{8}, \tfrac{1}{2}\underline{\gamma}, \tfrac{1}{2}\underline{\delta}\right\} > 0, \qquad \underline{\beta} = \min\left\{\tfrac{1}{8}, \tfrac{1}{2}(1 - \overline{\gamma}), \tfrac{1}{2}(1 - \overline{\delta})\right\} > 0,$$

where

$$\underline{\gamma} = \min_{i=0,\ldots,n} \gamma_i > 0, \qquad \overline{\gamma} = \max_{i=0,\ldots,n} \gamma_i < 1, \qquad \underline{\delta} = \min_{i=1,\ldots,n} \delta_i > 0, \qquad \overline{\delta} = \max_{i=1,\ldots,n} \delta_i < 1,$$

and

$$\alpha_i = \beta_i \in \left\{ \tfrac{1}{12}, \tfrac{1}{6}, \tfrac{1}{4}, \tfrac{1}{3} \right\}, \gamma_i = \tfrac{1}{2}$$
$$\Rightarrow \quad \delta_i = \tfrac{1}{2}$$

$$\alpha_i = \beta_i = \tfrac{1}{6}, \gamma_i \in \left\{ \tfrac{1}{8}, \tfrac{1}{2}, \tfrac{7}{8} \right\}$$
$$\Rightarrow \quad \delta_i \in \left\{ \tfrac{7-\sqrt{7}}{6}, \tfrac{1}{2}, \tfrac{\sqrt{7}-1}{6} \right\}$$

$$(\alpha_i, \beta_i, \gamma_i) \in \left\{ \left(\tfrac{1}{6}, \tfrac{1}{4}, \tfrac{3}{11} \right), \left(\tfrac{2}{5}, \tfrac{1}{5}, \tfrac{2}{3} \right), \left(\tfrac{5-i}{12}, \tfrac{i+1}{12}, \tfrac{5-i}{6} \right) \right\}$$
$$\Rightarrow \quad \delta_i \in \left\{ \tfrac{4}{7}, \tfrac{1}{2}, \tfrac{1}{2} \right\}$$

$$\alpha_i = \tfrac{1}{2}\gamma_i, \beta_i = \tfrac{1}{2}(1-\gamma_i), \gamma_i \in \left\{ \tfrac{1}{4}, \tfrac{1}{2}, \tfrac{3}{4} \right\}$$
$$\Rightarrow \quad \delta_i = \tfrac{1}{2}$$
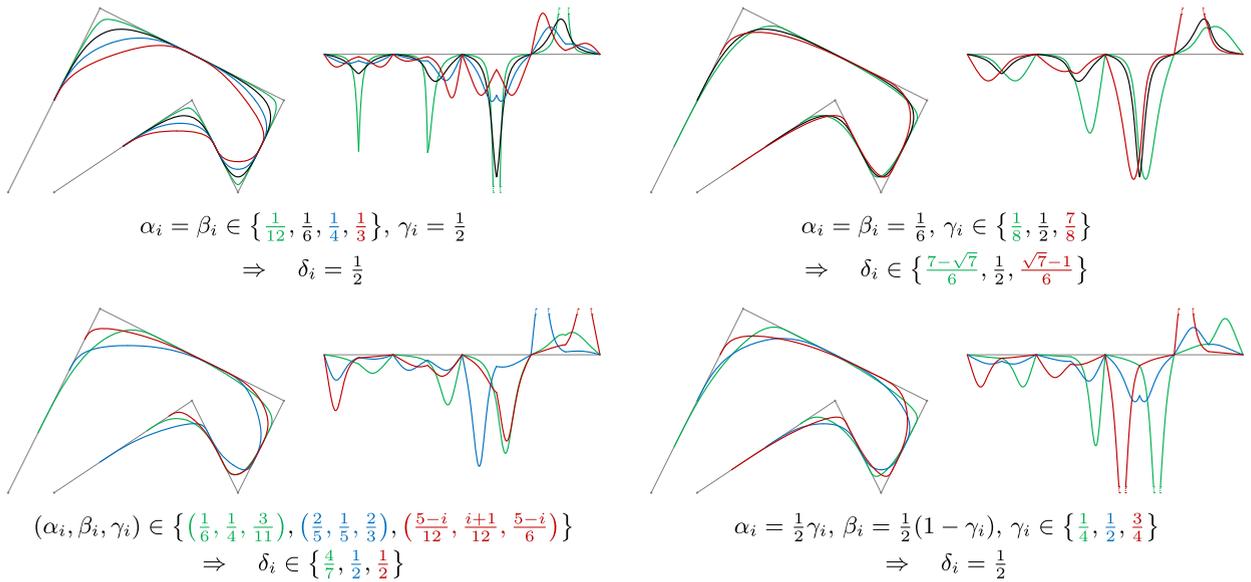
Fig. 7. Limit curve and signed curvature of the limit curve for the non-uniform corner cutting scheme with cut ratios in (18) for different choices of α_i, β_i, and γ_i. The black curves are the limit curves of the basic scheme (cf. Fig. 2, bottom). (For interpretation of the colours in the figure(s), the reader is referred to the web version of this article.)

$$\overline{\alpha} = \max\left\{ \tfrac{13}{40}, \tfrac{1}{2}\overline{\gamma}, \tfrac{1}{2}\overline{\delta} \right\} < \tfrac{1}{2}, \qquad \overline{\beta} = \max\left\{ \tfrac{13}{40}, \tfrac{1}{2}(1-\underline{\gamma}), \tfrac{1}{2}(1-\underline{\delta}) \right\} < \tfrac{1}{2}.$$

Hence, while the Gregory–Qu condition (4) for C^1 limit curves is not necessarily satisfied, the weaker condition (3) holds, and it is clear that the sequence (P_k) converges to a C^0 limit curve P.

Similar to Corollary 4, one can then show that P agrees with the Bézier spline B at all dyadic points in $[0, 2n]$ and must therefore be identical to B. The only changes in the arguments used in the proof of Corollary 4 regard the case p_1^{k+1}, where we now have $(1 - \gamma_0)\alpha_0^k = \gamma_0\beta_0^k$ and therefore $c_0 = (1 - \gamma_0)p_0^k + \gamma_0 p_1^k$ for $k \geq 1$, and the case $p_{2^k}^{k+1}$, where we need to ensure that $c_3 = (1 - \delta_1)p_{2^{k-1}}^k + \delta_1 p_{2^{k-1}+1}^k$. But the latter is true, because $(1 - \delta_1)\alpha_{2^{k-1}}^k = \delta_1\beta_{2^{k-1}}^k$ for $k \geq 1$. $\quad\square$

Fig. 7 illustrates the effect of the shape parameters α_i, β_i, and γ_i. On the one hand, α_i and β_i can be used to pull the limit curve towards the corners of the initial control polygon P_0. For example, if we set $\gamma_i = \tfrac{1}{2}$ and $\alpha_i = \beta_i = \zeta$ for all i and some $\zeta \in (0, \tfrac{1}{2})$, then we reproduce the limit curve of the basic scheme (see Fig. 2, bottom) for $\zeta = \tfrac{1}{6}$ and get limit curves that are closer to P_0 for $\zeta < \tfrac{1}{6}$ or further from P_0 for $\zeta > \tfrac{1}{6}$ (see Fig. 7, top left). On the other hand, γ_i specifies the point q_{2i} at which the limit curve touches the initial control polygon. For example, if we set $\alpha_i = \beta_i = \tfrac{1}{6}$ and $\gamma_i = \tfrac{1}{8}$ for all i, then the limit curve touches P_0 at the points $q_{2i} = \tfrac{7}{8}p_{2i}^1 + \tfrac{1}{8}p_{2i+1}^1 = \tfrac{3}{4}p_i^0 + \tfrac{1}{4}p_{i+1}^1$ (see Fig. 7, top right). While this restricts the touching points to be (strictly) between p_{2i}^1 and p_{2i+1}^1, we can also force the curve to pass through any point $q_{2i} = (1 - \zeta_i)p_i^0 + \zeta_i p_{i+1}^0$ that is (strictly) between p_i^0 and p_{i+1}^0 by setting $\gamma_i = \zeta_i \in (0, 1)$, $\alpha_i = \tfrac{1}{2}\zeta_i$, and $\beta_i = \tfrac{1}{2}(1 - \zeta_i)$. For example, the curves in Fig. 7 (bottom right) touch P_0 in the same points as the curves in Fig. 7 (top right), but the particularity of this second approach is that it gives $\delta_{i+1} = \tfrac{1}{2}$ for all i, hence the limit curve is guaranteed to touch the midpoints of the edges $[p_{2i+1}^1, p_{2i+2}^1]$. The latter can more generally by achieved by setting $\gamma_i = \alpha_i/(\alpha_i + \beta_i)$ (e.g., the blue and the red curve in Fig. 7, bottom left), and of course it is possible to mix these effects, to choose α_i and β_i asymmetrically, and to let them depend on the index i. In all cases the signed curvature plot confirms the G^2 continuity of the limit curve.

The Bézier spline B with control points in (17) can also be expressed as a non-uniform γ-B-spline (Boehm, 1985; Prautzsch et al., 2002, Section 7.4) $D : [u_0, u_{2n}] \rightarrow \mathbb{R}^2$ with knots $u_{-3}, u_{-2}, \ldots, u_{2n+3}$, chosen such that the ratios of the knot distances $\Delta_j = u_{j+1} - u_j$ for $j = -2, -1, \ldots, 2n + 1$ satisfy

$$\frac{\Delta_{2i}}{\Delta_{2i-1}} = \frac{1 - \gamma_i}{\gamma_i}, \qquad \frac{\Delta_{2i+1}}{\Delta_{2i}} = \frac{1 - \delta_{i+1}}{\delta_{i+1}}, \tag{20}$$

with arbitrarily chosen $\delta_0, \delta_{n+1} \in (0, 1)$, $2n + 3$ control points

$$d_{2i-1} = p_i^0, \qquad\qquad i = 0, \ldots, n + 1,$$
$$d_{2i} = (1 - \tau_i)p_i^0 + \tau_i p_{i+1}^0, \qquad i = 0, \ldots, n, \tag{21}$$
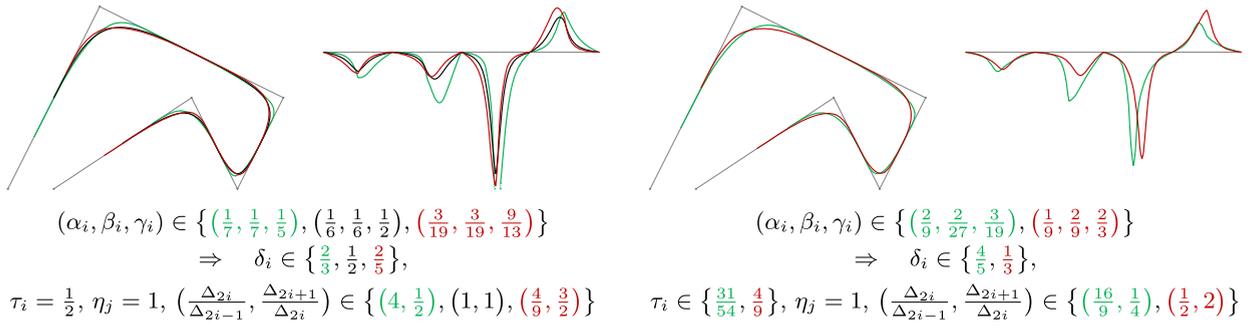
Fig. 8. Limit curve and signed curvature of the limit curve for the non-uniform corner cutting scheme with cut ratios in (18) for different choices of α_i, β_i, and γ_i, which all guarantee that the limit curve is a non-uniform cubic B-spline. The black curve is the limit curve of the basic scheme (cf. Fig. 2, bottom).

where $\tau_i = (1 + \alpha_i - \beta_i)/2$, and corresponding *tension parameters*[1]

$$\eta_{2i-1} = \frac{2\alpha_i}{\gamma_i(1 - \alpha_i - \beta_i)} \cdot \frac{1 - \delta_i}{\delta_i}, \qquad \eta_{2i} = 1, \qquad \eta_{2i+1} = \frac{2\beta_i}{(1 - \gamma_i)(1 - \alpha_i - \beta_i)} \cdot \frac{\delta_{i+1}}{1 - \delta_{i+1}} \qquad (22)$$

for $i = 0, \dots, n$. Note that the definition of δ_{i+1} in (14) guarantees that the definitions of η_{2i-1} for $i = 1, \dots, n$ and η_{2i+1} for $i = 0, \dots, n-1$ in (22) are equivalent, and that Δ_{-3} and Δ_{2n+2} can be chosen arbitrarily. As remarked by Boehm (1985), a non-uniform γ-B-spline is a non-uniform B-spline, if and only if all tension parameters are equal to one. Hence, it follows from (22) that the corner cutting scheme with cut ratios in (18) generates a non-uniform cubic B-spline in the limit for certain choices of α_i, β_i, and γ_i (see Fig. 8).

4. Piecewise rational limit functions

We can further extend our approach to generate piecewise rational G^2 splines as limit curves. More precisely, let us define, for any $r \geq 0$, the rational functions $R_0, R_1, R_2 : [0, 1] \to \mathbb{R}$,

$$R_0(t) = \frac{2t - rt + 2r}{2t - 2rt + 2r}(1 - t)^2, \qquad R_1(t) = \frac{4t - rt + 3r}{2t - 2rt + 2r}(1 - t)t, \qquad R_2(t) = \frac{2t}{2t - 2rt + 2r}t^2,$$

which simplify to the quadratic Bernstein polynomials for $r = 0$. Just like the latter, these functions are non-negative, form a partition of unity, and satisfy

$$R_0(0) = 1, \qquad R_1(0) = 0, \qquad R_2(0) = 0, \qquad R_0'(0) = -R_1'(0), \qquad R_2'(0) = 0,$$
$$R_0(1) = 0, \qquad R_1(1) = 0, \qquad R_2(1) = 1, \qquad R_0'(1) = 0, \qquad R_1'(1) = -R_2'(1).$$

It follows that the rational curve $S(t) = \sum_{m=0}^{2} s_m R_m(t)$ with control points $s_0, s_1, s_2 \in \mathbb{R}^2$ has the endpoint interpolation property, is tangent to the control edges $[s_0, s_1]$ and $[s_1, s_2]$ at $t = 0$ and $t = 1$, respectively, and is contained in the convex hull of its control points. If $r > 0$, then it is not hard to show that

$$S'(0) = \frac{3}{2}(s_1 - s_0), \qquad S'(1) = (r + 2)(s_2 - s_1),$$
$$S''(0) = \frac{1 - r}{r}(s_1 - s_0), \qquad S''(1) = 2(r^2 + r + 1)(s_2 - s_1) - (r + 2)(s_1 - s_0)$$

and that the signed curvature of S at the endpoints is

$$\kappa_S(0) = 0, \qquad \kappa_S(1) = \frac{\det(s_1 - s_0, s_2 - s_1)}{(r + 2)\|s_2 - s_1\|^3}. \qquad (23)$$

For $r = 1$, we note that $R_0 = B_0^3 + \frac{1}{2}B_1^3$, $R_1 = \frac{1}{2}B_1^3 + B_2^3$, and $R_2 = B_3^3$, where B_m^3 are the Bernstein polynomials of degree 3, and hence $S(t)$ is the cubic Bézier curve with control points s_0, $\frac{1}{2}(s_0 + s_1)$, s_1, s_2 in this special case.

We now consider the spline $S : [0, 2n] \to \mathbb{R}^2$ that consists of the $2n$ rational pieces $S_j : [j, j + 1] \to \mathbb{R}^2$, defined as

$$S_{2i}(t) = \sum_{m=0}^{2} s_m^{2i} R_m(t - 2i), \qquad S_{2i+1}(t) = \sum_{m=0}^{2} s_m^{2i+1} R_{2-m}(2i + 2 - t)$$

with control points

---

[1] As the name suggests, these tension parameters are commonly denoted by γ_i. Here we use η_i instead, because γ_i is already used for some of our shape parameters.

$$s_0^{2i} = q_{2i}, \qquad\qquad s_0^{2i+1} = q_{2i+1},$$
$$s_1^{2i} = p_{2i+1}^1, \qquad\qquad s_1^{2i+1} = p_{2i+2}^1, \tag{24}$$
$$s_2^{2i} = q_{2i+1}, \qquad\qquad s_2^{2i+1} = q_{2i+2},$$

for $i = 0, \dots, n-1$, where $p_0^1, \dots, p_{2n}^1$ and $q_1, \dots, q_{2n}$ are defined as in (15) and (16). By the remark above, S simplifies to the cubic Bézier spline B with control points in (17) for $r = 1$.

Proposition 9. *The piecewise rational spline S with control points in* (24) *is curvature continuous for any $r > 0$.*

Proof. Since s_1^{2i-1}, $s_2^{2i-1} = s_0^{2i}$, s_1^{2i} are collinear, it follows from (23) that the rational curves S_{2i-1} and S_{2i}, for $i = 1, \dots, n$, join curvature continuously with zero curvature. Moreover, for $i = 0, \dots, n-1$, the curves S_{2i} and S_{2i+1} join with G^1 continuity, because s_1^{2i}, $s_2^{2i} = s_0^{2i+1}$, s_1^{2i+1} are collinear. To verify that the joint is also G^2, it suffices to recall from Proposition 7 that this is true for $r = 1$ and from (23) that for any other $r > 0$ the curvature of both S_{2i} and S_{2i+1} at the joint is just the curvature in the special case $r = 1$, scaled by $3/(r+2)$. $\square$

To derive the appropriate cut ratios of the non-uniform corner cutting scheme that generates S in the limit, let us focus on the first piece of S, namely the rational curve $S(t) = \sum_{m=0}^{2} s_m R_m(t)$ with control points $s_0 = q_0$, $s_1 = p_1^1$, $s_2 = q_1$. By Proposition 1, the lines tangent to S at $S(t)$ and $S(t+h)$ intersect at $S(t) + \lambda_h S'(t)$ with

$$\lambda_h = \frac{\det\big(S(t+h) - S(t), S'(t+h)\big)}{\det\big(S'(t), S'(t+h)\big)}.$$

By the partition of unity property,

$$S(t) = s_1 + (s_0 - s_1)R_0(t) + (s_2 - s_1)R_2(t) \qquad\qquad S'(t) = (s_0 - s_1)R_0'(t) + (s_2 - s_1)R_2'(t),$$

so that

$$\lambda_h = \frac{(R_0(t+h) - R_0(t))R_2'(t+h) - (R_2(t+h) - R_2(t))R_0'(t+h)}{R_0'(t)R_2'(t+h) - R_2'(t)R_0'(t+h)},$$

which, after some simplifications, can be expressed as

$$\lambda_h = \frac{h(t - rt + r)\big((2t - 2rt + 3r)t + (2t - 2rt + 2r)h\big)}{(2t - 2rt + 3r)\big((2t - 2rt + 2r)t + (2t - 2rt + r)h\big)}.$$

As in the proof of Corollary 4 and Theorem 8, it then follows that the corner cutting scheme generates the intersection points of the tangent lines at $S\big(t_{i-1}^{k-1}\big)$ and $S\big(t_i^{k-1}\big)$ as p_i^k for $k \geq 1$, if we use the cut ratios

$$\alpha_i^k = \frac{\lambda_{-h} - \lambda_{-2h}}{\lambda_{2h} - \lambda_{-2h}}, \qquad\qquad \beta_i^k = \frac{\lambda_{2h} - \lambda_h}{\lambda_{2h} - \lambda_{-2h}} \qquad \text{with } h = \frac{1}{2^k} \text{ and } t = 2ih,$$

for $i = 1, \dots, 2^{k-1} - 1$, as well as

$$\alpha_0^k = \gamma_0 \frac{\lambda_h}{\lambda_{2h}}, \qquad\qquad \beta_0^k = (1 - \gamma_0)\frac{\lambda_h}{\lambda_{2h}} \qquad \text{with } h = \frac{1}{2^k} \text{ and } t = 0$$

and

$$\alpha_{2^{k-1}}^k = \delta_1 \frac{\lambda_{-2h} - \lambda_{-h}}{\lambda_{-2h}}, \qquad\qquad \beta_{2^{k-1}}^k = (1 - \delta_1)\frac{\lambda_{-2h} - \lambda_{-h}}{\lambda_{-2h}} \qquad \text{with } h = \frac{1}{2^k} \text{ and } t = 1.$$

Like before, the same cut ratios must be used for the points corresponding to the other pieces S_j of S with j even, while they need to be mirrored for the pieces S_j with j odd. Moreover, the parameter r can be replaced by a local parameter r_{i+1} for every pair of pieces (S_{2i}, S_{2i+1}), $i = 0, \dots, n-1$. After simplification, this gives the cut ratios

$$\alpha_i^k = \begin{cases} \alpha_i, & \text{if } k = 0, \\ \frac{1}{2}\gamma_{l_i^k - 1}, & \text{if } j_i^k = 0, \\ 2\delta_{l_i^k} \upsilon(-j_i^k, l_i^k), & \text{if } j_i^k = -2^{k-1}, \\ \omega(j_i^k, k, l_i^k), & \text{otherwise}, \end{cases} \qquad \beta_i^k = \begin{cases} \beta_i, & \text{if } k = 0, \\ \frac{1}{2}(1 - \gamma_{l_i^k - 1}), & \text{if } j_i^k = 0, \\ 2(1 - \delta_{l_i^k})\upsilon(-j_i^k, l_i^k), & \text{if } j_i^k = -2^{k-1}, \\ \omega(-j_i^k, k, l_i^k), & \text{otherwise}, \end{cases} \tag{25}$$

where

$$\upsilon(j, l) = \frac{2(2 + r_l)j^2 - 6j + (2 - r_l)}{2\big((2 + r_l)j - 2\big)\big(4j - (2 - r_l)\big)}$$

$$\alpha_i = \beta_i = \tfrac{1}{4}, \; \gamma_i = \tfrac{1}{2}, \; r_i \in \left\{8, \tfrac{1}{8}\right\}$$

$$\alpha_i = \tfrac{1}{6}, \; \beta_i = \tfrac{1}{4}, \; \gamma_i = \tfrac{3}{11}, \; r_i \in \left\{1, 2^{10-3i}\right\}$$
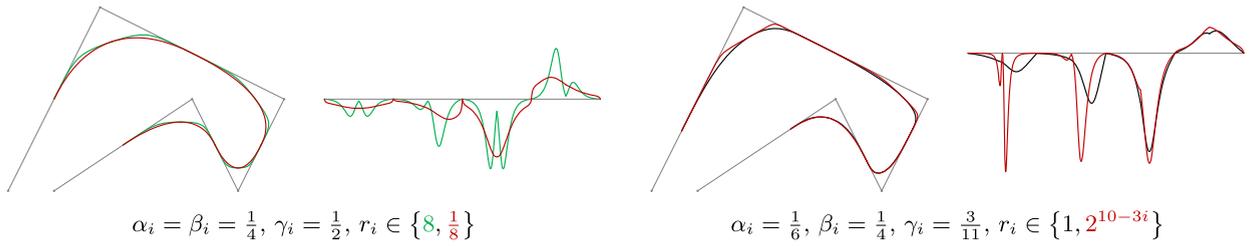
Fig. 9. Limit curve and signed curvature of the limit curve for the non-uniform corner cutting scheme with cut ratios in (25) for different choices of α_i, β_i, γ_i, and r_i. The black curve matches the green curve in Fig. 7 (bottom left).

and

$$\omega(j,k,l) = \frac{\left(2^k(6j^2 - 6j + 1)r_l + 4|j|(2j-1)(j-1)(1-r_l)\right)\left(2^k(2j+1)r_l + 4|j|(j+1)(1-r_l)\right)}{4\left(2^k(3j^2-1)r_l + 4|j|(j+1)(j-1)(1-r_l)\right)\left(2^k(4j-1)r_l + 4|j|(2j-1)(1-r_l)\right)},$$

and j_i^k and l_i^k are defined as in (6) and (19).

Fig. 9 illustrates the effect of the additional shape parameters r_i. Setting all $r_i = 1$ reproduces the Bézier splines from Section 3 in the limit, decreasing r_i pushes the limit curve away from p_{2i-1}^1 and p_{2i}^1, and increasing r_i has the opposite effect. As all $r_i \to \infty$, the limit curve converges to P_1, in contrast to the role of α_i and β_i, which can be used to let the limit curve converge to P_0 as all $\alpha_i, \beta_i \to 0$. Moreover, if $\alpha_i = \beta_i = \tfrac{1}{4}$ and $r_i \to 0$ for all i, then the limit curve converges to the quadratic B-spline (cf. Fig. 2, top) with only piecewise continuous curvature.

The rational spline S with control points in (24) can also be expressed as a non-uniform rational γ-B-spline (Boehm, 1987) $D : [u_0, u_{2n}] \to \mathbb{R}^2$ with knots $u_{-3}, u_{-2}, \ldots, u_{2n+3}$, chosen such that the ratios of the knot distances $\Delta_j = u_{j+1} - u_j$ for $j = -2, -1, \ldots, 2n + 1$ are as in (20), weights[2]

$$v_{6i-6} = 1, \quad v_{6i-5} = \frac{2r_i+1}{3r_i}, \quad v_{6i-4} = \frac{r_i+2}{3r_i}, \quad v_{6i-3} = \frac{1}{r_i}, \quad v_{6i-2} = \frac{r_i+2}{3r_i}, \quad v_{6i-1} = \frac{2r_i+1}{3r_i}, \quad v_{6i} = 1$$

for $i = 1, \ldots, n$, control points as in (21), where

$$\tau_i = \frac{1+\alpha_i-\beta_i}{2} + \frac{1-\alpha_i-\beta_i}{2}\left(2\gamma_i - 1 + \frac{(1-\gamma_i)^2 v_{6i-2}^2 - \gamma_i^2 v_{6i+2}^2}{(1-\gamma_i)v_{6i-2}^2 v_{6i+1} + \gamma_i v_{6i+2}^2 v_{6i-1}}\right)$$

with $v_{-2} = \frac{r_0+2}{3r_0}, v_{-1} = \frac{2r_0+1}{3r_0}, v_{6n+1} = \frac{2r_{n+1}+1}{3r_{n+1}}, v_{6n+2} = \frac{r_{n+1}+2}{3r_{n+1}}$ for any $r_0, r_{n+1} > 0$, and tension parameters

$$\eta_{2i-1} = \frac{1}{v_{6i-2}} \cdot \frac{2\alpha_i}{\gamma_i(1-\alpha_i-\beta_i)} \cdot \frac{1-\delta_i}{\delta_i},$$

$$\eta_{2i} = \frac{(1-\gamma_i)v_{6i-1} + \gamma_i v_{6i+1}}{(1-\gamma_i)v_{6i-2}^2 v_{6i+1} + \gamma_i v_{6i+2}^2 v_{6i-1}},$$

$$\eta_{2i+1} = \frac{1}{v_{6i+2}} \cdot \frac{2\beta_i}{(1-\gamma_i)(1-\alpha_i-\beta_i)} \cdot \frac{\delta_{i+1}}{1-\delta_{i+1}}$$

for $i = 0, \ldots, n$. Clearly, if all r_i are equal to one, then all weights v_j are equal to one, and the limit curve is a non-rational γ-B-spline. Moreover, the limit curve is C^2 if the tension parameters satisfy certain conditions (Boehm, 1987), that is, for specific choices of α_i, β_i, γ_i, and r_i.

5. Conclusion

The primary objective of this paper is to demonstrate that non-uniform corner cutting is capable of producing limit curves that are smoother than those generated by uniform corner cutting. In this sense, it complements the work by Dyn et al. (2022), who obtain a similar result for interpolatory 2-point and 4-point schemes, albeit with an entirely different approach. One may object that the schemes presented above generate only curves for which an analytic parametric representation is available, but we recall that the theory of uniform subdivision, apart from the pioneering work by de Rham (1947a,b, 1956, 1959), has similar origins. In fact, the topic became popular only with Chaikin's (re-)discovery of the corner cutting scheme for quadratic B-splines (Chaikin, 1974) and the subsequent generalization for obtaining uniform B-splines of arbitrary degree via subdivision (Lane and Riesenfeld, 1980), that is, with schemes that generate known limit curves.

---

[2] These are the rational weights associated with the $6n + 1$ Bézier control points of the $2n$ rational cubic pieces of D.

However, we are aware of the fact that the real challenge lies in identifying non-uniform corner cutting schemes for curvature continuous limit curves that are not known *a priori*, and further exploration is needed to develop suitable tools for analysing such schemes, which go beyond the well-established methods of asymptotic equivalence (Dyn and Levin, 1995; Dyn et al., 2014), asymptotic similarity (Conti et al., 2015), and proximity (Wallner and Dyn, 2005; Wallner, 2006). Our first experiments in this direction indicate that this will be very challenging. Whereas the smoothness of uniform subdivision schemes is usually quite stable with respect to small modifications of the weights of the rules, as long as the weights continue to sum to one, it seems as if the curvature continuity of the limit curves obtained from the corner cutting schemes above is lost as soon as just a single cut ratio α_i^k or β_i^k is perturbed slightly. This shows that it is not sufficient to guarantee a certain limit behaviour of the cut ratios as $k \to \infty$, but that most probably a more holistic condition needs to be satisfied, which involves the cut ratios for all k and all i.

CRediT authorship contribution statement

Kai Hormann: Writing – review & editing, Writing – original draft, Formal analysis. **Claudio Mancinelli:** Writing – review & editing, Writing – original draft, Formal analysis.

Declaration of competing interest

The authors declare that they have no known competing financial interests or personal relationships that could have appeared to influence the work reported in this paper.

Data availability

No data was used for the research described in the article.

References

Boehm, W., 1985. Curvature continuous curves and surfaces. Comput. Aided Geom. Des. 2, 313–323. https://doi.org/10.1016/S0167-8396(85)80006-6.

Boehm, W., 1987. Rational geometric splines. Comput. Aided Geom. Des. 4, 67–77. https://doi.org/10.1016/0167-8396(87)90025-2.

de Boor, C., 1987. Cutting corners always works. Comput. Aided Geom. Des. 4, 125–131. https://doi.org/10.1016/0167-8396(87)90029-X.

de Boor, C., 1990. Local corner cutting and the smoothness of the limiting curve. Comput. Aided Geom. Des. 7, 389–397. https://doi.org/10.1016/0167-8396(90)90002-9.

Chaikin, G.M., 1974. An algorithm for high-speed curve generation. Comput. Graph. Image Process. 3, 346–349. https://doi.org/10.1016/0146-664X(74)90028-8.

Conti, C., Dyn, N., Manni, C., Mazure, M.L., 2015. Convergence of univariate non-stationary subdivision schemes via asymptotic similarity. Comput. Aided Geom. Des. 37, 1–8. https://doi.org/10.1016/j.cagd.2015.06.004.

Dyn, N., Hormann, K., Mancinelli, C., 2022. Non-uniform interpolatory subdivision schemes with improved smoothness. Comput. Aided Geom. Des. 94, 102083. https://doi.org/10.1016/j.cagd.2022.102083.

Dyn, N., Levin, D., 1995. Analysis of asymptotically equivalent binary subdivision schemes. J. Math. Anal. Appl. 193, 594–621. https://doi.org/10.1006/jmaa.1995.1256.

Dyn, N., Levin, D., Yoon, J., 2014. A new method for the analysis of univariate nonuniform subdivision schemes. Constr. Approx. 40, 173–188. https://doi.org/10.1007/s00365-014-9247-1.

Fang, M.e., Jeong, B., Yoon, J., 2017. A family of non-uniform subdivision schemes with variable parameters for curve design. Appl. Comput. Math. 313, 1–11. https://doi.org/10.1016/j.amc.2017.05.063.

Farin, G., 2002. Curves and Surfaces for CAGD: A Practical Guide. The Morgan Kaufmann Series in Computer Graphics and Geometric Modeling, 5th ed. Morgan Kaufmann, San Francisco.

Goldman, R., 2003. Pyramid Algorithms: A Dynamic Programming Approach to Curves and Surfaces for Geometric Modeling. The Morgan Kaufmann Series in Computer Graphics and Geometric Modeling. Morgan Kaufmann, San Francisco.

Gregory, J.A., Qu, R., 1996. Nonuniform corner cutting. Comput. Aided Geom. Des. 13, 763–772. https://doi.org/10.1016/0167-8396(96)00008-8.

Jeong, B., Yang, H., Yoon, J., 2021. A non-uniform corner-cutting subdivision scheme with an improved accuracy. J. Comput. Appl. Math. 391, 113446. https://doi.org/10.1016/j.cam.2021.113446.

Lane, J.M., Riesenfeld, R.F., 1980. A theoretical development for the computer generation and display of piecewise polynomial surfaces. IEEE Trans. Pattern Anal. Mach. Intell. 2, 35–46. https://doi.org/10.1109/TPAMI.1980.4766968.

Paluszny, M., Prautzsch, H., Schäfer, M., 1997. A geometric look at corner cutting. Comput. Aided Geom. Des. 14, 421–447. https://doi.org/10.1016/S0167-8396(96)00038-6.

Prautzsch, H., Boehm, W., Paluszny, M., 2002. Bézier and B-Spline Techniques. Mathematics and Visualization. Springer, Berlin.

de Rham, G., 1947a. Un peu de mathématiques à propos d'une courbe plane. Elem. Math. II, 73–76.

de Rham, G., 1947b. Un peu de mathématiques à propos d'une courbe plane (suite). Elem. Math. II, 89–97.

de Rham, G., 1956. Sur une courbe plane. J. Math. Pures Appl. 35, 25–42.

de Rham, G., 1959. Sur les courbes limites de polygones obtenus par trisection. Enseign. Math. V, 29–43. https://doi.org/10.5169/seals-35472.

Riesenfeld, R.F., 1975. On Chaikin's algorithm. Comput. Graph. Image Process. 4, 304–310. https://doi.org/10.1016/0146-664X(75)90017-9.

Wallner, J., 2006. Smoothness analysis of subdivision schemes by proximity. Constr. Approx. 24, 289–318. https://doi.org/10.1007/s00365-006-0638-3.

Wallner, J., Dyn, N., 2005. Convergence and C^1 analysis of subdivision schemes on manifolds by proximity. Comput. Aided Geom. Des. 22, 593–622. https://doi.org/10.1016/j.cagd.2005.06.003.